Supplement of Atmos. Chem. Phys., 20, 3879–3893, 2020
https://doi.org/10.5194/acp-20-3879-2020-supplement

Atmospheric Chemistry and Physics
Open Access
EGU

Supplement of

Effect of inorganic-to-organic mass ratio on the heterogeneous OH reaction rates of erythritol: implications for atmospheric chemical stability of 2-methyltetrols

Rongshuang Xu et al.

Correspondence to: Man Nin Chan (mnchan@cuhk.edu.hk)

Molecular Dynamics (MD) Simulation

To gain more insights into the effect of ammonium sulfate (AS) on the reactive OH uptake process, all-atom MD simulations of the OH radical impinging particles were carried out in the two particles setups shown in Table S1 and Scheme S1 and S2. OpenMM v7.3 (Eastman et al., 2017) was used to perform the MD simulations. The general AMBER force field (GAFF) (Wang et al., 2004) was adopted for the erythritol, OH radical, ammonium, and sulfate ions. The water model was SPC/E model (Berendsen et al., 1987). Water molecules and all the chemical bonds connected to hydrogen atoms were kept rigid. R. E. D.-III 5.2 tools (Dupradeau et al., 2010) were used to calculate the RESP partial charges in GAFF.

For each simulation, a particle was placed at the origin of a nonperiodic simulation box. A flat-bottomed restraining potential was applied to keep the atoms inside the box:

$$V(r) = k(r-d)^2 H(r-d) \quad \text{(S1)}$$

where r is the radial distance of the atom from the origin, k is the force constant and was set to be 10 kcal mol^{-1} nm^{-2}. $H(\cdot)$ is the Heaviside step function. d was set to be 0.2 nm larger than the particle radius at the beginning of the equilibration. All the intermolecular interactions were calculated explicitly without any cutoffs. For equilibration in each setup, the particle was first run under constant *NVT* (constant number of particles, volume, and temperature) dynamics with a time step of 2 fs at 300 K for 500 ps. Then, the system was slowly heated up to 1000 K at a rate of 1 K ps^{-1} and was kept at 1000 K for 4 more ns. The temperature was slowly cooled down to 300 K at a rate of –1 K ps^{-1} and was kept at 300 K for 6 more ns with d (in the restraining potential) set to be 6.5 nm before the impinging simulations. In each impinging simulation, one OH radical was placed randomly on a spherical surface with a radius of 4.0 nm (setup I) or 4.5 nm (setup II) from the particle center. The OH radical was

assigned an initial velocity v_0, whose magnitude was chosen to be the root-mean-square speed of the Maxwell-Boltzmann distribution at 300 K, towards the particle center. The impinging simulations were performed under constant *NVE* (*E* for energy) dynamics with a time step of 1 fs to study the dynamical process of gas uptake. 500 independent trajectories of 100 ps were collected for each setup.

Table S1. Particles setups in the MD simulations.

	setup I		setup II	
System	Pure erythritol (IOR = 0)		Erythritol-AS particles (IOR =1)	
label	No ion		$(NH_4)_2SO_4$ & more water	
radius (nm)	2.2		2.9	
particle composition	weight percentage (wt %)	number of molecules	weight percentage (wt %)	number of molecules
Water	52.7	1000	60.9	2700
Erythritol	47.3	132	20.3	132
$(NH_4)_2SO_4$	0	0	18.8	113

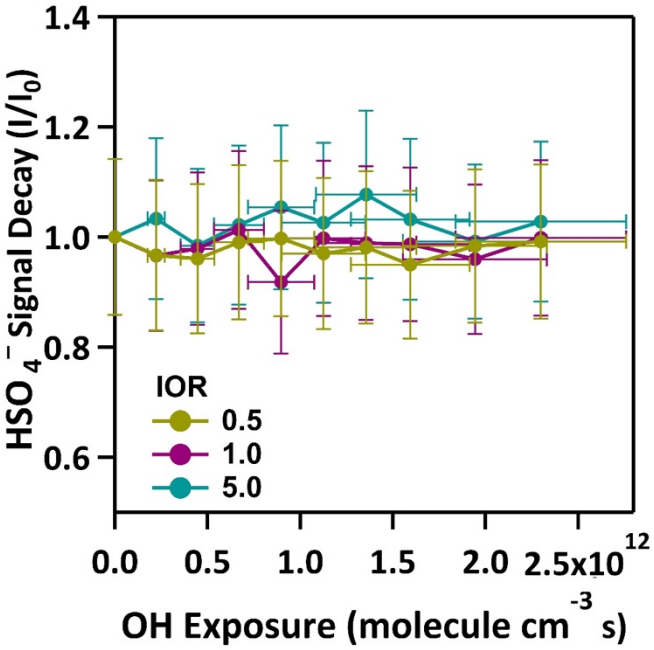

Figure S1. The relative change of the bisulfate (HSO_4^-) ion intensity for erythritol-AS particles as a function of OH exposure.

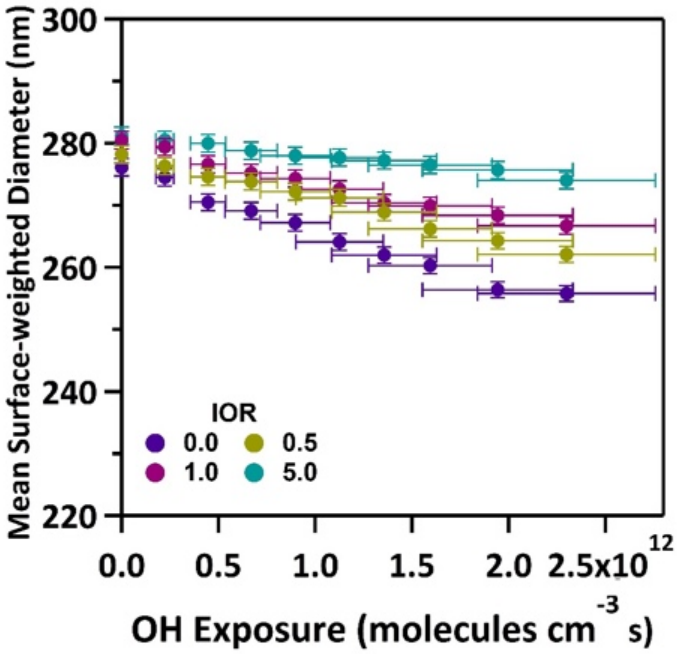

Figure S2. The change in surface-weighted mean diameter as a function of OH exposure for erythritol particles and erythritol-AS particles with different IORs.

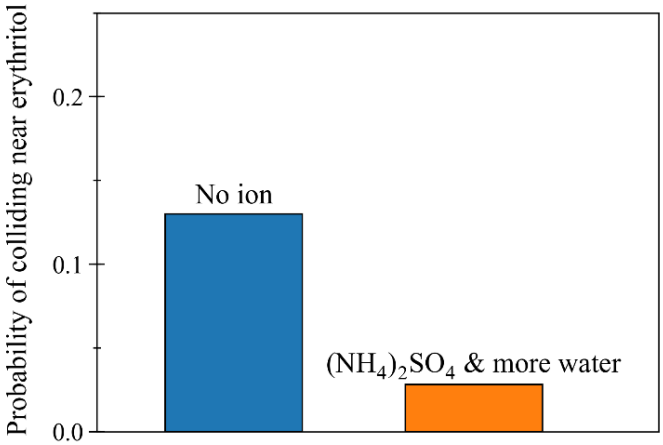

Figure S3. Probability of OH colliding near the erythritol molecules at first impact estimated from all the impinging trajectories. The distance cutoff was chosen to be 3 Å.

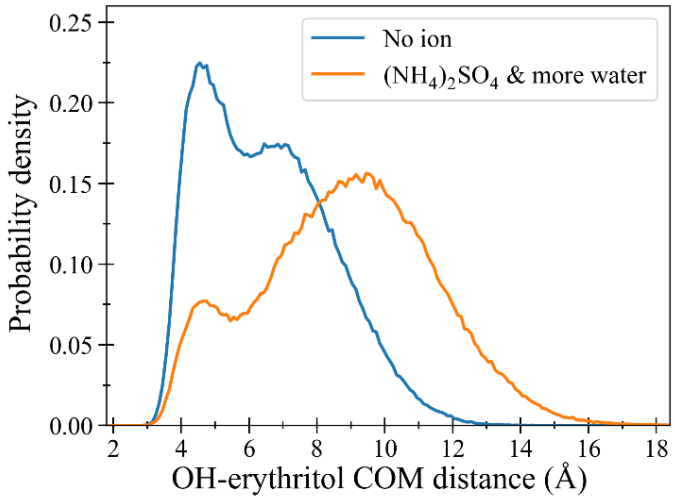

Figure S4. Probability densities of the distance between OH and its nearest erythritol neighbor after gas adsorption. First 20 ps data were excluded to eliminate any possible nonequilibrium effects after gas adsorption.

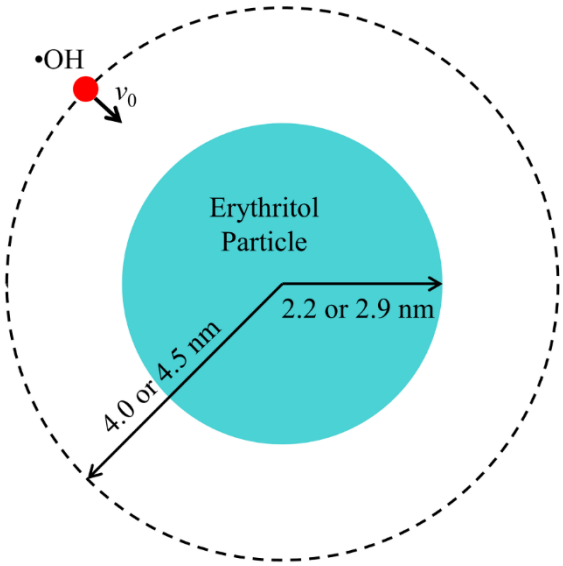

Scheme S1. The setup of impinging simulations.

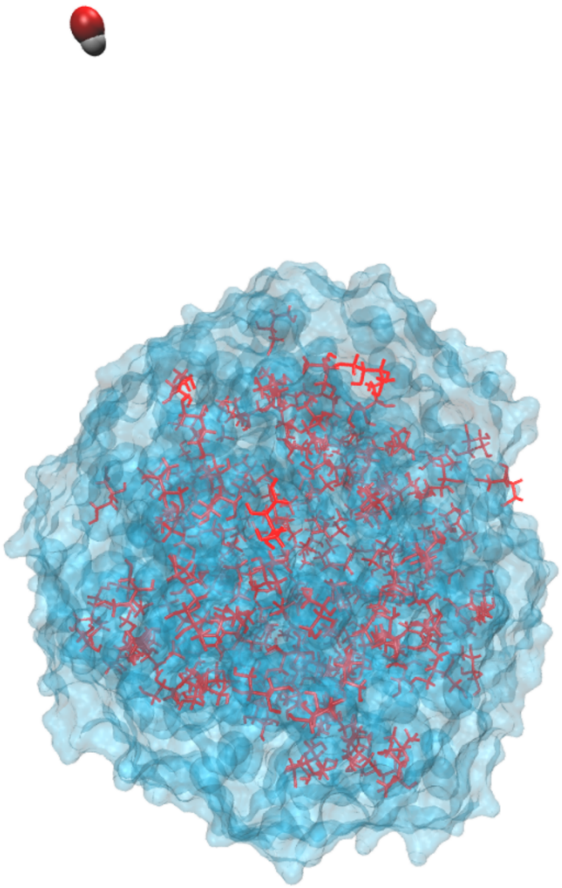

Scheme S2. Snapshot of the initial configuration of an impinging simulation. All the solutes are shown in red lines.

References

Berendsen, H. J. C., Grigera, J. R. and Straatsma, T. P.: The missing term in effective pair potentials, J. Phys. Chem., 91, 6269–6271, doi:10.1021/j100308a038, 1987.

Dupradeau, F.-Y., Pigache, A., Zaffran, T., Savineau, C., Lelong, R., Grivel, N., Lelong, D., Rosanski, W. and Cieplak, P.: The R.E.D. tools: advances in RESP and ESP charge derivation and force field library building, Phys. Chem. Chem. Phys., 12, 7821, doi:10.1039/c0cp00111b, 2010.

Eastman, P., Swails, J., Chodera, J. D., Mcgibbon, R. T., Zhao, Y., Beauchamp, K. A., Wang, L.-P., Simmonett, A. C., Harrigan, M. P., Stern, C. D., Wiewiora, R. P., Brooks, B. R. and Pande, V. S.: OpenMM 7: Rapid development of high performance algorithms for molecular dynamics, PLoS Comput. Biol., 13, doi:10.1371/journal.pcbi.1005659, 2017.

Wang, J., Wolf, R. M., Caldwell, J. W., Kollman, P. A. and Case, D. A.: Development and testing of a general amber force field, J. Comput. Chem., 25, 1157–1174, doi:10.1002/jcc.20035, 2004.